Available online at www.sciencedirect.com
ScienceDirect
Journal of Photochemistry and Photobiology A: Chemistry 186 (2007) 342–348
Journal of Photochemistry and Photobiology A:Chemistry
www.elsevier.com/locate/jphotochem

Solution medium effects on the photochemical degradation of pyrene in water

Catherine D. Clark *, Warren J. De Bruyn, Jackie Ting, William Scholle

Department of Physical Sciences, Chapman University, One University Drive, Orange, CA 92866, United States

Received 30 June 2006; received in revised form 24 August 2006; accepted 1 September 2006
Available online 18 October 2006

Abstract

Poly-aromatic hydrocarbons (PAHs), carcinogenic compounds ubiquitous in the environment, are readily degraded photochemically. Understanding the kinetics and mechanisms of their photochemical degradation is important in assessing their overall toxicity. Here we have measured the photo-oxidation rate of pyrene in aqueous solution as a function of environmentally relevant solution media. The degradation rate of pyrene is $0.268\,min^{-1}$ in air-equilibrated water at pH 8. Degradation appears to require water and is dependant on oxygen concentrations, ionic strength and the concentration of humic acid in solution. Rates decrease as oxygen concentrations decrease, reaching a rate of $0.0424\,min^{-1}$ in argon-purged solutions. Degradation increases as ionic strength increases and decreases as humic acid concentration increases. Rates will vary by as much as an order of magnitude over the range of environmental ionic strengths and humic acid concentrations. Mechanistic studies showed the formation of the 1-hydroxypyrene intermediate, consistent with a previously proposed mechanism in the literature that proceeds via electron transfer from excited singlet state pyrene to oxygen.

Keywords: Pyrene; Photodegradation; Water; Oxygen; Humic acid

1. Introduction

Poly-aromatic hydrocarbons (PAHs), a group of carcinogenic compounds produced in the incomplete combustion of biomass and fossil fuels, are widely distributed in the environment and have been designated as priority pollutants [1,2]. PAHs are ubiquitous in urban atmospheres and are frequently found in rivers, lakes, sediments and particulate matter downwind of urban areas [3–10]. Sources of PAHs in urban areas include forest fires, coal processing and use/combustion of fossil fuels for domestic heating, industrial processes and transportation. PAHs enter the atmosphere directly as gas-phase species or as primary aerosol emissions. Once in the atmosphere, PAHs partition between the gas phase and particulate phase depending on temperature, available particulate surface area and volatility [11]. PAHs enter surface waters directly from surface runoff and atmospheric deposition [12,13]. Aerosols are also believed to be a significant source of high molecular weight PAHs to surface waters. Sediments may be a significant source of PAHs to overlying waters, particularly where inputs to the sediment have been high due to pollution or petroleum seeps. Low molecular weight PAHs are more likely to collect in the aqueous phase than higher molecular weight compounds, which collect in soils and sediments [14].

Over the last 30 years, there have been measurements of PAH concentrations in rivers, lake waters, aerosols and sediments (see for example, [3–5,7,9,10,15]) with levels occasionally exceeding the Environmental Protection Agency's (EPA) standard [16] for total PAH in surface waters [10]. However, the chemistry of these species in the environment is poorly understood. Because degradation of PAHs can produce toxic/carcinogenic products [17,18] we need to understand the chemistry of these species in the environment in order to understand their overall toxicity. An understanding of the degradation chemistry is also central to developing effective remediation strategies. Since PAHs absorb light strongly in the ultraviolet region, PAHs in the environment will undergo photochemical reactions,

* Corresponding author. Tel.: +1 714 628 7341; fax: +1 714 532 6048.
E-mail address: cclark@chapman.edu (C.D. Clark).

1010-6030/$ – see front matter © 2006 Elsevier B.V. All rights reserved.
doi:10.1016/j.jphotochem.2006.09.003

including photo-dimerization and photo-oxidation [17–19]. To ultimately understand the fate and transport of PAHs in the environment, it is therefore critical to establish a solid understanding of the kinetics and mechanisms of PAH photochemistry.

A number of recent studies have focused on the photo-oxidation of PAHs in aquatic systems [20–24]. These studies have shown that many of the higher molecular weight polycyclic aromatics are rapidly transformed in water by sunlight [21], rates tend to increase with molecular weight [21,22], and degradation follows first-order kinetics, with the extent of photodegradation often increasing with increasing oxygen concentration, temperature, illumination and exposure time [20–24]. Reported quantum yields vary by as much as a factor of 2 [21–24] and the mechanism for aquatic photo-oxidation is not clear. Zepp and Schlotzhauer [21] measured the photodegradation of 12 PAHS in de-gassed versus air-saturated solvents and suggested that the primary photochemical process in water was direct photolysis and did *not* involve O_2. But Mill et al. [24] found that purging aqueous PAH samples with oxygen increased photolysis, suggesting that oxygen does play a critical role. One proposed mechanism is energy transfer from the excited aromatic triplet state to an oxygen molecule to give singlet oxygen, which then reacts with the PAH to give peroxides and quinones [22]. More recently, Sigman et al. [23] also found that oxygen was important but suggested that the first step in the photochemical oxidation of pyrene is electron transfer from the excited singlet state of pyrene to molecular oxygen and 1,6- and 1,8-pyrenequinones are formed as stable products, with 1-hydroxypyrene as an intermediate. The same photoproducts have also been detected as major products in photochemical studies of pyrene absorbed onto surfaces in air-equilibrated water [25–27].

Very little is known about how degradation rates vary as a function of natural water solution media (e.g. ionic strength, humic acid concentration, etc.). Zepp et al. [28] showed that first-order rate constants for photo-oxidation of an organic aromatic compound were directly proportional to concentrations of humic acid (complex biologically produced organic molecules found in natural waters). A recent review concluded that there are no detailed data on the influence of inorganic salts on the photodegradation of PAHs in water, and more information is needed on the effects of dissolved organic material on these processes [20].

A study of the mechanism and kinetics of pyrene photodegradation in aqueous solutions as a function of solution medium is reported here. Pyrene was chosen as the model PAH for this study because of its solubility in water due its relatively small four-ring size, and its presence in natural water systems. Mechanistic studies involved product identification, measurement of apparent first-order rate constants in the presence and absence of water and oxygen, and the comparison of data with a numerical model based on a proposed mechanism in the literature [23]. Kinetic studies were performed in aqueous solutions as a function of varying ionic strength and humic acid concentrations to elucidate pyrene photodegradation rates and half-lives in a range of natural waters.

2. Materials and methods

2.1. Reagents

Deionized water was obtained from distilled water run through a Barnstead ion-exchange system (Model D8961). For photochemical rate studies in water, 1.26 g of pyrene (Tokyo Kasei Kogyo Co. Ltd.) was dissolved in acetonitrile (ACN, HPLC grade, Burdick & Jackson) in a 100 mL volumetric flask to give a 0.0625 M pyrene stock solution. An aliquot of 0.1 mL of this concentrated stock solution was diluted with ACN to 100 mL to give a 62.5 μM dilute stock solution. The dilute stock solution was further diluted with deionized water to give 250 mL of 0.625, 0.3125, 0.0625, and 0.0344 μM pyrene solutions for calibrating the HPLC. The 0.625 μM pyrene solution was used for irradiations. The highest concentration of pyrene in water was 0.625 μM because the maximum solubility of pyrene in water is 0.653 μM (0.135 mg L^{-1}) [29]. For photochemical product identification studies by HPLC using 3-D UV/VIS detection, a more concentrated solution of 50 μM pyrene was made up in 30% ACN/water (v/v) solution, because of the need for higher absorbance and the solubility limit of pyrene in pure water. To test the effect of the absence of water from the solution medium, a 50 μM pyrene solution was made up in 100% ACN. To test the effect of oxygen, samples were purged with 99.999% pure argon gas (Airgas; 10 PSI) for 60 min prior to the irradiation, with continued purging during the irradiations. Purging for time periods shorter than 40 min resulted in increased rates, likely due to residual oxygen.

NaCl (35.0311 g, Fisher Scientific) was dissolved in deionized water in a 250 mL volumetric flask to give a 2.39 M NaCl stock solution. The NaCl stock solution was diluted with 0.1 mL of 62.5 μM pyrene stock solution and deionized water in 10 mL volumetric flasks to give 0.001, 0.01, 0.1, 0.5, and 1.0 M NaCl solutions containing 0.625 μM of pyrene. The pH of a stock 0.625 μM pyrene solution was adjusted from pH 8 to 1 and 2 using 6 M HCl (VWR) for pH experiments. A standard humic acid (Aldrich) was dissolved with deionized water to give a 50.0 mg L^{-1} humic acid stock solution. The humic acid stock solution was diluted with 0.1 mL of 62.5 μM pyrene stock solution and deionized water in 10 mL volumetric flasks to give 1.0, 5.0, 10.0, 20.0 and 50.0 mg L^{-1} humic acid solutions containing 0.625 μM of pyrene.

All solutions were wrapped with aluminum foil and kept in a cabinet in the dark.

2.2. Photochemical irradiations

Solutions were irradiated in 1 cm × 1 cm quartz cells with a septa cap. One cell filled with deionized water was placed in front of the sample cell as an IR filter. A 200 W xenon/mercury lamp (Oriel Instruments, Model 6292) was used as the light source. A cooling fan (Radio Shack) placed at 90 degrees to the side was used to cool the sample cell. The temperature of deionized water inside the sample cell was monitored with a digital thermometer as a function of irradiation time. With the IR filter and cooling fan the temperature inside the sample cell

increased by less than 1.5 °C within 5 min of irradiation, and remained constant throughout the remainder of the irradiation time up to 60 min. The xenon lamp was allowed to stabilize for 20 min before irradiations. Samples (220 μL) were removed from the irradiation cell at different times during the irradiation and analyzed by HPLC [30]. Three trials were performed for each experiment. For solutions irradiated in the absence of oxygen, samples were purged in the sample cell for 60 min prior to the irradiation and during the irradiation with argon gas. A 1 mL aliquot of a 0.625 μM pyrene aqueous solution was placed in a small wrapped vial in a cabinet as a dark control before each irradiation. Pyrene-free solvents were also irradiated to determine if the solvents had any appreciable photochemistry. Dark controls and solvent blank irradiations were analyzed by HPLC prior to pyrene irradiations. In all irradiations dark controls and irradiated water and solvent blanks showed no significant photochemistry within the 2–5% analytical error of the experiment.

2.3. HPLC analysis

An Agilent HPLC 1100, equipped with UV–vis diode-array and fluorescence detectors, 200 μL manual injector, a 25 cm × 2.1 mm LC-PAH column (Supelco), and ChemStation software 4.0, was used to analyze pyrene and its photoproducts. The mobile phase was a mixture of 10% water/90% ACN (v/v). The column flow rate was ramped from an initial flow rate of 0.2 to 1 mL min^{-1} after 2 min and the temperature of the column was set at 26 °C. Under these conditions pyrene eluted at approximately 2.7 min. The injection loop was flushed with 20 mL of ACN before and after each analysis. The column was conditioned for 30 min with the mobile phase while the detector lamps were stabilized before the experiment.

The UV–vis diode array detector was used for photoproduct time course experiments. Absorbance was measured from 200 to 400 nm as a function of retention time. To allow for the relatively high detection limits needed in this mode, experiments were carried out with a concentrated 50 μM solution of pyrene in 30% ACN/water (v/v). The detector was calibrated for pyrene with standard solutions of 1–50 μM pyrene solutions in 30% acetonitrile and concentrations of pyrene were determined from integrated peak areas using ChemStation 4.0 software. The concentration of a proposed intermediate 1-hydroxypyrene was determined from molar extinction coefficients measured independently on an Agilent 8453 UV/VIS spectrometer.

Because of the lower concentrations of pyrene in aqueous solution, pyrene was analyzed by fluorescence intensity (λ_{ex} = 238 nm, λ_{em} = 398 nm) rather than absorbance. Detection limits were 0.00625 μM. The fluorescence detector was calibrated for pyrene using standard solutions of 0.625, 0.3125, 0.0625, and 0.0344 μM pyrene in water. Pyrene concentrations were once again determined from integrated peak areas using ChemStation 4.0 software. The precision of the HPLC was routinely checked with a 0.625 μM pyrene standard solution injection before each experiment and typically ranged from 2 to 5%.

2.4. GC/MS analysis

To aid product analysis, 10 irradiations were carried out in a larger 10 cm path length quartz cell and irradiated solutions combined and analyzed by solid-phase extraction GC/MS. A combined irradiated solution (100 mL) was loaded onto a Supelco ENVI-18 solid-phase extraction cartridge at a flow rate of ∼10 mL min^{-1}. Prior to extraction, the cartridge was conditioned with 26.0 mL of toluene: methanol (10:1, v/v) solution, 6.0 mL of methanol and 6.0 mL of deionized water. After loading, the cartridge was air dried for 10.0 min and the pyrene and oxidation products eluted with 21.0 mL of toluene:methanol (10:1, v/v) solution. A 5 μL aliquot of the resultant solution was injected directly onto a CP-SIL 8 column (Varian: 30 × 25 × 0.25) and analyzed by Ion Trap Mass Spectrometry (Varian Saturn 2200) using EPA method 525. Hydroxypyrene was identified by mass spectrum using the Varian mass spectrum library.

3. Results and discussion

3.1. Mechanistic studies

Pyrene rapidly underwent photolysis on irradiation in the presence of oxygen, following apparent first-order kinetics with a slope of 0.268 min^{-1} (Fig. 1). First-order kinetics have been previously observed for PAH photolysis, with the extent of photodegradation increasing with increasing oxygen concentration, temperature, illumination and exposure time [20]. In a typical experiment in this work, pyrene concentrations decreased by a factor of ∼100 within 10 min of irradiation. A previous estimated half-life for the photolysis of pyrene by sunlight is 0.68 h, and quantum yields reported in the literature range from 0.0021 to 0.0041 [21,24]. The half-life in this study using a higher intensity xenon lamp is 0.043 h or 2.59 min and an approximate quantum yield based on lamp specifications from the manufacturer

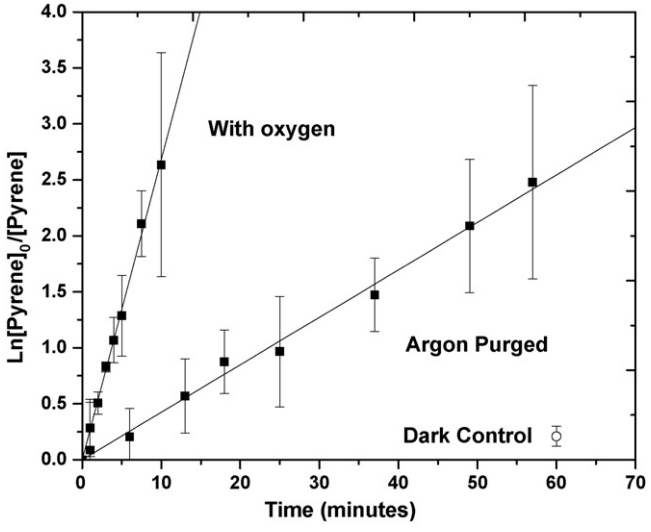

Fig. 1. First-order plots of pyrene concentrations as a function of irradiation time (in min) for air-equilibrated and argon-purged aqueous solutions.

is consistent with the above range. The concentration of dissolved oxygen in air-equilibrated aqueous solutions at 25 °C is 2.68×10^{-4} M [31].

In argon-purged solutions, the photolysis again followed apparent first-order kinetics but with a rate ~6× slower (slope = 0.0424 min^{-1}), with a decrease in pyrene concentration by a factor of ~10 in 60 min (Fig. 1). The half-life of pyrene was 16.3 min. By contrast, Sigman et al. [23] show a smaller difference of a factor of 4 in the rates between their air-equilibrated and argon-purged solutions. Purging for a shorter period of time in this study (20 min versus 60 min) resulted in an increase in the apparent first-order rate by a factor of 2, giving results similar to the Sigman et al. study [23].

These results show that oxygen plays an important role in the mechanism of pyrene photochemistry in aqueous medium. This is consistent with the work of Mill et al. [24] and Sigman et al. [23] and is not consistent with the observations made by Zepp and Schlotzhauer [21]. This suggests that the mechanism is not direct photolyisis. Both an energy transfer, singlet oxygen–pyrene mechanism [24] and the electron transfer from an excited singlet state of pyrene to molecular oxygen mechanism proposed by Sigman et al. [23] would explain an oxygen-dependant degradation rate.

In 30% ACN/water (v/v) solutions, the apparent first-order rate constants were on the same order as those measured for aqueous solutions. 3D UV/VIS analysis of reactants and products showed that an intermediate (retention time (RT) = 1.03 min) is initially rapidly formed on a timescale of 5 min as pyrene is depleted, followed by a slower transformation of the intermediate into two final products on a timescale of 8–20 min (overlapping peaks and RT = 1.45 min). HPLC retention time, absorbance/fluorescence characteristics, and GC/MS analysis identified the intermediate as 1-hydroxypyrene. In the absence of water in 100% ACN solutions, this intermediate was not detected in air-equilibrated and argon-purged solutions, although degradation did occur on a much slower timescale (by two orders of magnitude). This suggests that water is also a reactant in the mechanism in aqueous solutions. These observations are consistent with the mechanism proposed by Sigman et al. [23]. As shown in Scheme 1, the Sigman et al. [23] mechanism involves a pyrene radical cation water trapping step and the primary intermediate is 1-hydroxypyrene. Once again this is not consistent with direct photolysis. It is also not consistent with an energy transfer, singlet oxygen–pyrene mechanism which would produce peroxides and quinones [24].

To test the Sigman et al. [23] mechanism, experimental reaction and product concentrations were compared to the output of a numerical model (Fig. 2). Pyrene concentrations were determined from integrated peak areas. Hydroxypyrene concentrations were approximated from absorbance peak heights at 205 nm and molar extinction coefficients determined independently. The quinone product concentration was approximated assuming that the absorption coefficient of the quinone is the same as the hydroxypyrene (the quinone was not available). Sigman et al. [23] suggested the final products are 1,6- and 1,8-pyrenequinone. These two quinones could not be resolved so they have been treated as a single quinone product. Where possible rate constants are those suggested by Sigman et al. [23]. k_1 was determined directly from the observed first-order loss of pyrene. Step 4, the protonation of Py-OH was assumed to be negligible based on the starting pH of 8. k_3 and k_8, the deprotonation of the pyrene radical cation and the photolysis of the hydroxypyrene intermediate, were adjusted to give the best fit to the hydroxypyrene intermediate data. The quinone data was not

Step 1: Electron transfer	$[Pyrene.O_2] \rightarrow Pyrene^{\cdot+} + O_2^{\cdot-}$	k_1
Step 2: Ring addition of water	$Pyrene^{\cdot+} + H_2O \rightarrow Py\text{-}H_2O^{\cdot+}$	k_2
Step 3: Deprotonation	$Py\text{-}H_2O^{\cdot+} \rightarrow Py\text{-}OHH + H^+$	k_3
Step 4: Reverse of Step 3	$Py\text{-}OHH + H^+ \rightarrow Py\text{-}H_2O^{\cdot+}$	k_4
Step 5: Removal of H^+	$O_2^{\cdot-} + H^+ \rightarrow H_2O$	k_5
Step 6: Reverse of Step 5	$H_2O \rightarrow O_2^{\cdot-} + H^+$	k_6
Step 7: Formation of intermediate	$Py\text{-}OHH + O_2 \rightarrow$ 1-hydroxypyrene	k_7
Step 8: Rearrangement to products	1-hydroxypyrene→1,6 + 1,8-pyrenequinone	k_8

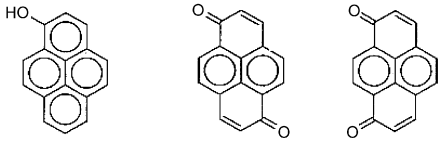

Intermediate
1-hydroxypyrene

Products
1,6- and 1,8-pyrenequinones

Scheme 1. Proposed reaction mechanism for the photochemical degradation of pyrene in air-equilibrated aqueous solutions (adapted from [23]).

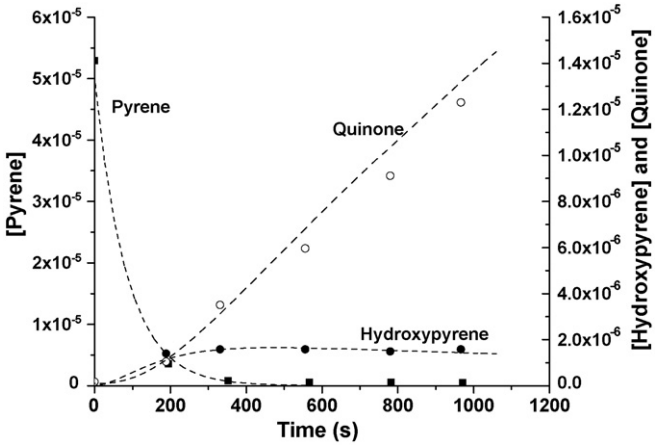

Fig. 2. Comparison of modeled and experimental concentrations of pyrene, intermediate and products as a function of irradiation time (in s): model - - -; pyrene (■); 1-hydroxypyrene (●); quinone products (◯).

used to constrain the model because uncertainties in the concentrations are larger than the uncertainties in the hydroxypyrene data, given that the extinction coefficient for the quinone product was unknown. The agreement between model and data for the quinone suggests that the molar extinction coefficient for the quinone is probably similar to that for the hydroxypyrene at 205 nm. Final rate constants used are given in Table 1. The two photochemical processes, Steps 1 and 8, have similar rates suggesting that if these two processes have similar quantum yields as measured by Sigman et al. [23] then the integrated absorption coefficient for pyrene and hydroxypyrene over the 250–400 nm wavelength range would be similar in magnitude. Overall the model agrees reasonably well with the data, suggesting that the mechanism proposed by Sigman et al. [23] is consistent with the data in this experiment. Based on these experiments and the modeling results, the mechanism of pyrene photodegradation in air-equilibrated aqueous solutions appears to proceed via transfer of an electron from photo-excited pyrene to oxygen.

3.2. Solution medium effects

To examine the effect of varying salinity and levels of colored dissolved organic matter in natural water environments ranging from fresh to estuarine, the kinetics were measured as a function of ionic strength, pH and humic acid concentration. Rate constants are given in Table 2.

Table 1
Values for rate constants used in numerical model

Rate constant	Value
k_1	$1.2 \times 10^{-2}\ s^{-1}$
k_2	$2.2 \times 10^{6}\ s^{-1}$
k_3	$3.7 \times 10^{-4}\ s^{-1}$
k_4	$1.0 \times 10^{-3}\ M^{-1}\ s^{-1}$
K_a[a]	2.5×10^{-5}
k_7	$1.0 \times 10^{8}\ M^{-1}\ s^{-1}$
k_8	$1.2 \times 10^{-2}\ s^{-1}$

[a] Individual rate constants k_5 and k_6 not known; K_a from [23]. Varying k_5 and k_6 had little effect on the model output.

Table 2
Rate constants and half-lives for pyrene photodegradation in aqueous solutions as a function of ionic strength, pH and humic acid (HA) concentration

Solution	Rate constant (min^{-1})	Half-life (min)
Oxygen	0.268	2.59
Argon-purged	0.0424	16.3
0.001 M NaCl	0.242	2.86
0.01 M NaCl	0.296	2.34
0.1 M NaCl	0.510	1.36
0.5 M NaCl	0.168	5.95
1.0 M NaCl	0.151	6.62
pH 1	0.476	1.46
pH 2	0.285	2.43
0 mg L^{-1} HA	0.183	3.79
1 mg L^{-1} HA	0.190	3.65
5 mg L^{-1} HA	0.158	4.39
10 mg L^{-1} HA	0.145	4.78
20 mg L^{-1} HA	0.0935	7.49
50 mg L^{-1} HA	0.0572	12.1

(1) The humic acid experiments were conducted at a later time with a lower intensity lamp, and have lower apparent first-order rate constants (uncorrected for changing lamp intensity). (2) The average dark control rate constant was $0.004 \pm 0.002\ min^{-1}$.

3.2.1. Ionic strength and pH effects

To test the effect of ionic strength, experiments were repeated in air-equilibrated aqueous solutions in the presence of oxygen in different concentrations of NaCl. The apparent first-order rate constant initially increased linearly with increasing ionic strength from $I = 0.001$ to 0.1 M (Fig. 3). The half-life decreases by a factor of 2 from 2.86 min at $I = 0.001$ M to 1.36 min at $I = 0.1$ M. The nature of the solution affects electron transfer reaction rates by controlling the rate of diffusion and by establishing the microscopic environment of the solvent cage, within which the electron transfer between two species takes place [32]. The ionic strength effect observed here would be consistent with a rate determining step in the mechanism that involves two charged species diffusing together, or alternatively an effect

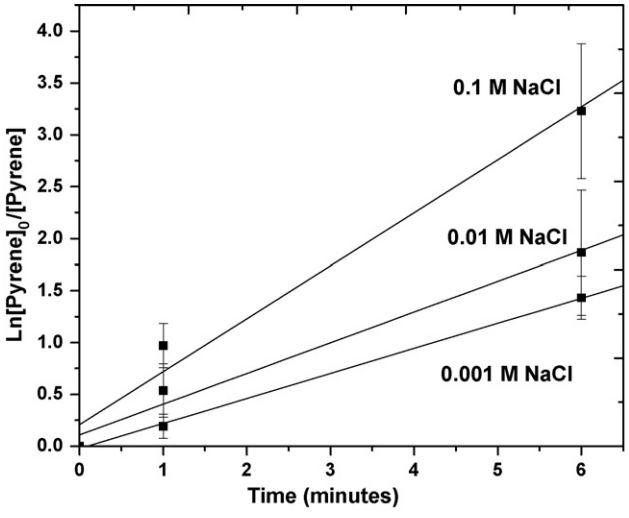

Fig. 3. First-order plots of pyrene concentrations as a function of irradiation time (in min) for air-equilibrated aqueous solutions with varying NaCl concentrations.

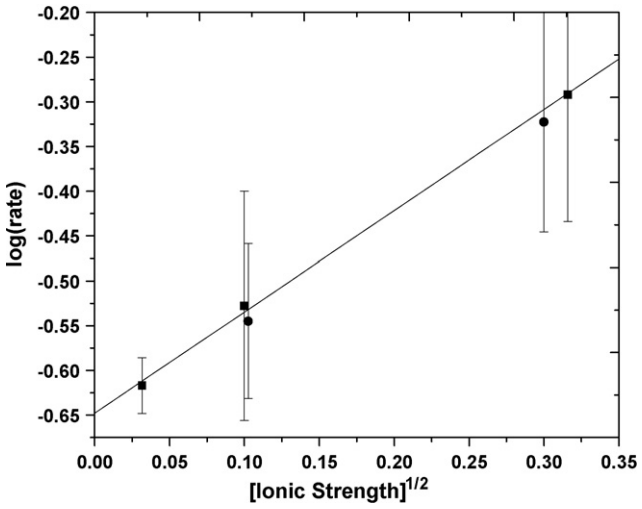

Fig. 4. Log of the apparent first-order rate constants (in min^{-1}) for pyrene photodegradation in air-equilibrated aqueous solutions as a function of the square root of ionic strength (M): NaCl (■); HCl (●).

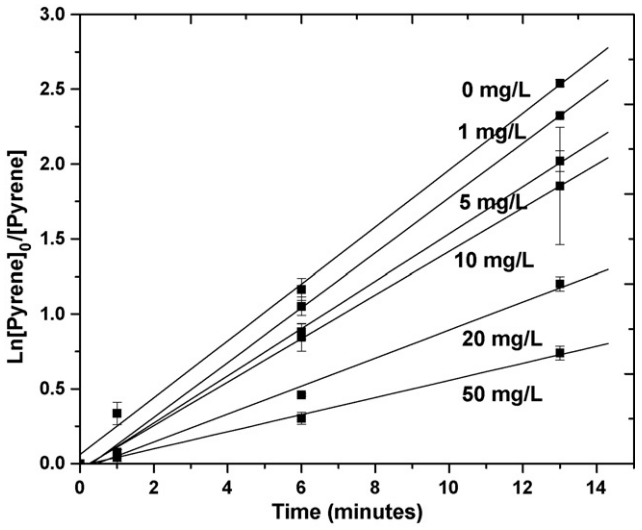

Fig. 5. First-order plots of pyrene concentrations as a function of irradiation time (in min) for air-equilibrated aqueous solutions with varying humic acid concentrations.

through solvent cage pairing [32]. Since the rate determining step according to the modeling results is most likely Step 3 (Scheme 1), which involves a neutral species separating from a H^+ ion, the effect observed here is likely due to the solvent cage environment. The equilibrium constant for the formation of ion pairs between charged species and counter ions in solution decreases with increasing ionic strength [32]. However, at higher ionic strengths of 0.5–1.0 M, the rate constant decreases to 0.15 min^{-1} and the half-life increases to 4.62 min (Table 2). This may be due to the deviation of activity coefficients from predicted behavior, with the activity coefficients decreasing linearly in regions of low ionic strength as I increases but then increasing as I continues to increase in regions of high ionic strength ($I > 0.6$ M for 1:1 electrolyte) [33].

The rate constants increased slightly by 10% from pH 8 to 2, but increased by a factor of 170% from pH 2 to 1. These pH trends are consistent with an ionic strength effect, with the acidified solutions correlating with salt solutions at an equivalent ionic strength for a plot of $\log k$ versus $I^{1/2}$ (Fig. 4). Since both the NaCl and HCl are 1:1 salts, the same concentration of chloride ion would result from solutions with the same ionic strength. Olson and Simonson reported that variations in rate constants were almost exclusively due to the concentration and nature of the counter ions in a kinetic salt effect, rather than ionic strength [32]. They explained the overall rate constant as being made up of contributions from the fraction of the species that is ion paired and the fraction of species that is not ion paired. This would lead to changes in the rate constant as the equilibrium constant for ion pairing varies with increasing ionic strength.

The ionic strength of seawater is 0.7 M, largely consisting of NaCl with some other salts, ranging down to values as low as 0.02 M for fresh riverine waters [31]. This corresponds to a variation in salinity from 36 down to <1. This variation in salinity could have an effect of as much as a factor of 2 on pyrene photodegradation rates, with the shortest half-lives predicted in estuarine waters with mid-range salinities from 10 to 20, corresponding to ionic strengths of ~0.1 M.

3.2.2. *Effect of humic acid*

To test the effect of humic acid, experiments were repeated in aqueous solutions in the presence of oxygen in different concentrations of humic acid solutions. As the concentration of humic acid was increased from 1 to 20 mg L^{-1}, the apparent first-order rate constant for the photodegradation of pyrene decreased linearly from 0.183 to 0.0935 min^{-1} (Fig. 5). The half-lives ranged from 3.79 to 7.49 min. However, at the highest concentration of 50 mg L^{-1}, the apparent first-order rate constant had stabilized at ~0.0572 min^{-1}, near the apparent first-order rate constant of 0.0424 min^{-1} in the argon-purged solutions (Fig. 6).

This could be due to absorption of the light by the humic acid, reducing pyrene photodegradation rates. However, based

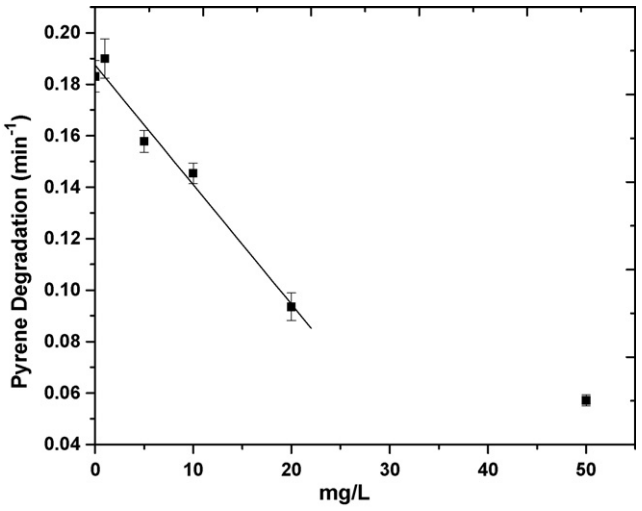

Fig. 6. Apparent first-order rate constants (in min^{-1}) for pyrene photodegradation in air-equilibrated aqueous solutions as a function of humic acid concentration (in mg L^{-1}).

on absorbance and concentrations, the relative light absorption by pyrene exceeds that of the humic acid by two to three orders of magnitude, so it is unlikely that this is a light reduction effect. This is more likely to be due to the adsorption of pyrene within the complex humic acid matrix, protecting it from oxygen and photodegradation. Pyrene has previously been shown to be rapidly and strongly absorbed to Aldrich humic acid in a study of the sorption of pollutants onto soils [34]. Humic acids have also been shown to increase the apparent water solubility of pyrene due to sorption in a micelle-like partition model [35]. Previous studies on the photochemical kinetics of pyrene absorbed to cellulose surfaces also showed decreased rate constants, attributed to the reduction in exposure of pyrene to oxygen within the cellulose matrix [27]. Therefore, the presence of humic acid in natural waters would act to slow the photochemical degradation of pyrene in water, potentially increasing its half-life by a factor of 4 from low DOM-containing ocean waters compared to high DOM-containing riverine and wetland waters.

4. Conclusions

Our results show that the photolysis of pyrene is substantially faster in the presence of oxygen and also requires water. Mechanistic studies showed the formation of the 1-hydroxypyrene intermediate, consistent with a previously proposed mechanism in the literature that proceeds via electron transfer from excited singlet state pyrene to oxygen. The photodegradation of pyrene is increased by a factor of 2 in weakly ionic solutions, but is decreased by a factor of 4 in humic acid containing solutions. Our results indicate that the half-life of pyrene in the environment will vary depending on the salinity and DOM composition of the water body, and may potentially vary by almost an order of magnitude for higher salinity lower DOM coastal waters versus lower salinity higher DOM river and lake waters.

Acknowledgements

The authors gratefully acknowledge the support of the donors of the American Chemical Society's Petroleum Research Fund (Grant # 36187 GB-4), the American Chemical Society's Project SEED program, and Chapman University's Faculty Scholarly/Creative Activity and Student Research Grant program. The authors thank Eli Morey, Joshua Jones, Daniel Wellman and Project SEED Summer Fellow Jessica Reveles (Orange High School) for assistance.

References

[1] B.P. Dunn, in: A. Bjorest (Ed.), Handbook of Polynuclear Aromatic Hydrocarbons, Marcel Dekker, New York, 1983.
[2] M.L. Lee, M.B. Novatny, K.D. Bartle, Analytical Chemistry of Polycyclic Aromatic Hydrocarbons, Academic Press, New York, 1981.
[3] J.J. Stegman, in: H.V. Gelboin, P.O. P Tso (Eds.), Polycyclic Hydrocarbons and Cancer, vol. 1, Academic Press Inc., New York, 1981, pp. 1–60.
[4] J. Borneff, H. Kunte, in: A. Bjorseth (Ed.), Handbook of Polycyclic Aromatic Hydrocarbons, Marcel Dekker, New York, 1983 (Chapter 15).
[5] E.F. Corcoran, M.S. Brown, F.R. Baddour, S.A. Chasens, A.D. Freay. Biscayne Bay Hydrocarbon Study, Final Report. State of Florida Department of Natural Resources, St. Petersburg, Florida, 1983.
[6] A. Bjorseth, T. Ramdahl, Handbook of Polycyclic Aromatic Hydrocarbons, 2, Marcel Dekker, New York, 1985.
[7] J.P. Meador, J.E. Stein, W.L. Reichert, U. Varanasi, Rev. Environ. Contam. Toxicol. 143 (1999) 79–165.
[8] G. Sanders, J. Hamilton-Taylor, K. Jones, Environ. Sci. Technol. 30 (1996) 2958–2966.
[9] E. Long, Sediment toxicity in Biscayne Bay, in: Proceedings of the Workshop on Toxic Materials in Biscayne Bay II: Assessment of Problems, Existing Data and Future Needs, RSMAS, University of Miami, 1998.
[10] S.M. Rudnick, R.F. Chen, Talanta 47 (1998) 907–919.
[11] T.F. Bidleman, Environ. Sci. Technol. 22 (1988) 361–367.
[12] D.L. Leister, J.E. Baker, Atmos. Environ. 28 (1994) 1499–1520.
[13] D. Golomb, D. Ryan, N. Eby, J. Underhill, T. Wade, S. Zemba, Atmos. Environ. 31 (1997) 1361–1368.
[14] M. Howsam, K.C. Jones, in: A.H. Neilson (Ed.), PAHs and Related Compounds: Chemistry, Springer, Berlin, 1998, pp. 138–173.
[15] J.O. Allen, N.M. Dookeran, K.A. Smith, A.F. Sarofim, K. Taghizadeh, A.L. Lafleur, Environ. Sci. Technol. 30 (1996) 1023–1031.
[16] Environmental Protection Agency, 1980. Document Ambient Water Quality Criteria for PAH.
[17] S. Belkin, M. Stieber, A. Thiem, F.H. Friemel, A. Abelovich, P. Werner, S. Ulitzur, Environ. Toxicol. Water Qual. 9 (1994) 303–309.
[18] R. Dabestani, I.N. Ivanov, Photochem. Photobiol. 70 (1999) 10–34.
[19] R.G. Harvey, in: A.H. Neilson (Ed.), Environmental Chemistry of PAHs. PAHs and Related Compounds: Chemistry, Springer, Berlin, 1998, pp. 2–53.
[20] J. Kochany, R.J. Maguire, Sci. Total Environ. 144 (1994) 17–31.
[21] R.G. Zepp, P.F. Schlotzhauer, in: P.W. Jones, P. Leber (Eds.), Polynuclear Aromatic Hydrocarbons, Ann Arbor Science Publishers, Ann Arbor, MI, 1979, pp. 141–158.
[22] M. Zander, in: A. Bjorseth (Ed.), Handbook of Polycyclic Aromatic Hydrocarbons, Marcel Dekker, New York, 1983 (Chapter 1).
[23] M.E. Sigman, P.F. Schuler, M.M. Ghosh, R.T. Dabestani, Environ. Sci. Technol. 32 (1998) 3980–3985.
[24] T. Mill, W.R. Mabey, B.Y. Lan, A. Baraze, Chemosphere 10 (1981) 1281–1290.
[25] C.A. Reyes, M. Medina, C. Crespo-Hernandez, M.Z. Cedeno, R. Arce, O. Rosario, D.M. Steffenson, I.N. Ivanov, M.E. Sigman, R. Dabestani, Environ. Sci. Technol. 34 (2000) 415–421.
[26] S. Wen, J.C. Zhao, G.Y. Sheng, J.M. Fu, P.A. Peng, Chemosphere 50 (2003) 111–119.
[27] A.S. Oliveira, L.F.V. Ferreira, J.P. Da Silva, J.C. Moreira, Int. J. Photoenergy 6 (2004) 205–213.
[28] R.G. Zepp, G.L. Baughman, P.F. Schlotzhauer, Chemosphere 10 (1981) 119–126.
[29] W.E. May, in: L. Petrakis, F.T. Weiss (Eds.), Petroleum in the Marine Environment, American Chemical Society, Washington, DC, 1980, pp. 68–82.
[30] D.L. Poster, L.C. Sander, S.A. Wise, in: A.H. Neilson (Ed.), PAHs and Related Compounds: Chemistry, Springer, Berlin, 1998, pp. 78–135.
[31] A.G. Howard, Aquatic Environmental Chemistry, Oxford University Press, New York, 1998, p. 10.
[32] C.D. Clark, M.Z. Hoffman, Coord. Chem. Rev. 159 (1997) 359–373.
[33] T. Engel, P. Reid, Thermodynamics, Statistical Thermodynamics and Kinetics, Pearson-Cummings, NY, 2006, p. 233.
[34] M.J. Simpson, A.J. Simpson, P.G. Hatcher, Environ. Toxicol. Chem. 23 (2004) 355–362.
[35] M. Fukushima, K. Oba, S. Tanaka, K. Nakayasu, H. Nakamura, K. Hasebe, Environ. Sci. Technol. 31 (1997) 2218–2222.